Studies of the magnetic structure at the ferromagnet - antiferromagnet interface

A. Scholl[1], F. Nolting[1,2], J. Stöhr[2,3], J. Lüning[2], J.W. Seo[4,5], J.-P. Locquet[5],

J. Fompeyrine[5], S. Anders[1,3], H. Ohldag[1,2,6], and H.A. Padmore[1]

[1]Advanced Light Source, 1 Cyclotron Road, Lawrence Berkeley National Laboratory, Berkeley, CA 94720, USA

[2]Stanford Synchrotron Radiation Laboratory, P.O. Box 20450, Stanford, CA 94309, USA

[3]IBM Research Division, Almaden Research Center, 650 Harry Road, San Jose, CA 95120, USA

[4]Institute de Physique, University of Neuchâtel, CH-2000 Neuchâtel, Switzerland

[5]IBM Research Division, Zürich Research Laboratory, CH-8803, Rüschlikon, Switzerland

[6]Institute of Applied Physics, University of Düsseldorf, Universitätsstr. 1, 40225 Düsseldorf, Germany

Abstract:

Antiferromagnetic layers are a scientifically challenging component in magneto-electronic devices such as magnetic sensors in hard disk heads, or magnetic RAM elements. In this paper we show that photo-electron emission microscopy (PEEM) is capable of determining the magnetic structure at the interface of ferromagnets and antiferromagnets with high spatial resolution (down to 20 nm). Dichroism effects at the L edges of the magnetic 3d transition metals, using circularly or linearly polarized soft x-rays from a synchrotron source, give rise to a magnetic image contrast. Images, acquired with the PEEM2 experiment at the Advanced Light Source, show magnetic contrast for antiferromagnetic $LaFeO_3$, microscopically resolving the magnetic domain structure in an antiferromagnetically ordered thin film for the first time. Magnetic coupling between $LaFeO_3$ and an adjacent Co layer results in a complete correlation of their magnetic domain structures. From field dependent measurements a unidirectional anisotropy resulting in a local exchange bias of up to 30 Oe in single domains could be deduced. The elemental specificity and the quantitative magnetic sensitivity render PEEM a perfect tool to study magnetic coupling effects in multi-layered thin film samples.

Introduction:

Anisotropy, confinement and interface effects completely alter the magnetic properties of thin magnetic films, enabling the engineer to design improved magnetic materials with novel properties. The surface and interface anisotropy is an important factor influencing the magnetic symmetry of thin films (Gradmann, 1991, Stöhr, 1999). Dimensionality effects control ordering parameters such as the Curie temperature in ferromagnets or the Néel temperature in antiferromagnets approaching monolayer thickness (Alders *et al.*, 1998, Schneider *et al.*, 1990). Magnetic exchange coupling and spin transport at interfaces are responsible for technologically important effects such as magnetic interlayer coupling, spin-tunneling, and giant magneto-resistance (Fert *et al.*, 1995). These effects are applied in technologically relevant devices such as magnetic sensors in hard disk read heads or magnetic random access memory (MRAM), generally referred to as spintronics applications. X-ray techniques are widely used, because of their high and quantitative magnetic sensitivity utilizing magnetic x-ray dichroism, and their elemental specificity (Kortright *et al.*, 1999). The variable probing depth of x-ray absorption by variation of the detected particles such as transmitted or reflected photons, fluorescence photons, low-energy secondary electrons or photo-electrons, allows the study of surface, interface or bulk effects.

In particular, we have investigated the magnetic structure of antiferromagnetic thin films and the phenomenon of exchange bias at the ferromagnet (FM) – antiferromagnet (AFM) interface using x-ray photo-electron emission microscopy (PEEM) (Nolting *et al.*, 2000, Scholl *et al.*, 2000, Stöhr *et al.*, 1999). Exchange bias or magnetic pinning occurs when a

FM and an AFM layer are grown adjacent to each other in an applied magnetic field resulting in a unidirectional magnetic anisotropy or a shift of the magnetic hysteresis loop of the FM (Berkowitz & Takano, 1999, Nogues & Schuller, 1999). Pinned magnetic layers serve as magnetic reference layers in magneto-electronic devices, utilizing the insensitivity of AFMs to magnetic fields. The microscopic origin of exchange bias is still poorly understood, largely due to the lack of techniques capable of providing information about the arrangement of spins at FM – AFM interfaces.

Experiment:

Samples consisting of an antiferromagnetic $LaFeO_3$ layer and a ferromagnetic Co layer, grown on a $SrTiO_3$ substrate, were investigated. The $LaFeO_3$ films were grown in an oxide molecular beam epitaxy (MBE) system by means of a block-by-block growth method (Locquet *et al.*, 1994) at 750°C under a beam of atomic oxygen and a partial O_2 pressure of 5×10^{-6} Torr. This method yields high-quality epitaxial films (Locquet *et al.*, 1998). The Co layers have been grown on $LaFeO_3$ by MBE without breaking the vacuum and were protected from oxidation by a 10 Å thick Pt coating.

The experimental setup is shown in the top right part of Fig. 1 (Anders *et al.*, 1999). Monochromatized x-rays from bending magnet beam line 7.3.1.1 of the Advanced Light Source illuminate the sample under an angle of incidence of 30°. The x-ray polarization can be easily varied from right circular to left circular and linear by moving an aperture in the beam line. We have exploited the polarization dependence of x-ray absorption in magnetic materials investigating the antiferromagnet $LaFeO_3$ using x-ray magnetic linear dichroism (XMLD) and the ferromagnet Co using x-ray magnetic circular dichroism (XMCD). The electric field vector for linearly polarized light lies in the sample plane. The all electrostatic PEEM2 microscope images low-energy, secondary photoelectrons from the sample with magnification onto a phosphor screen, which is read by a CCD camera. The spatial resolution of PEEM2 is limited by chromatic aberrations to 20 nm. A small electromagnet mounted on the sample puck was used to magnetize the sample in fields up to 0.02 T parallel to the surface.

Results:

Our experiments make use of the large XMLD effect previously observed in α-Fe$_2$O$_3$ (Kuiper *et al.*, 1993). The magnetic contribution to the temperature and polarization dependence of the Fe L-edge resonance intensity is proportional to $(3\cos^2\theta - 1)\langle M^2 \rangle_T$, where θ is the angle between the x-ray polarization vector $\vec{E}$ and the magnetic axis $\vec{A}$, and M is the magnetic moment operator (Alders *et al.*, 1998, Stöhr *et al.*, 1999). Thus, x-ray absorption spectroscopy is sensitive to the orientation of the antiferromagnetic axis $\vec{A}$ within an AFM domain relative to the x-ray polarization. In particular, peak A of the Fe L$_2$ edge at 721.5 eV is larger than peak B at 723.2 eV (see Fig. 1 inset) for $\vec{E} \perp \vec{A}$ and smaller for $\vec{E} \parallel \vec{A}$. The antiferromagnetic domains can be directly observed by combining XMLD spectroscopy with PEEM microscopy, that is by dividing a PEEM image acquired at 723.2 eV (image B) by one obtained at 721.5 eV (image A). The divided XMLD image B/A in Fig. 1 shows the antiferromagnetic domain structure of LaFeO$_3$, with domains with $\vec{E} \parallel \vec{A}$ appearing brighter than domains with $\vec{E} \perp \vec{A}$.

The angular dependence of the XMLD image contrast is visualized in Fig. 2. Two SrTiO$_3$ substrate crystals were joined macroscopically at (110) and (010) faces, leading to a 45° rotation of the lattice around the surface normal. Crystallographic twins in each half have an orthogonal orientation of the crystallographic c-axes, which lie in the sample plane, observed by transmission electron microscopy and x-ray diffraction. The crystallographic c-axes of these twins are oriented along the diagonals on the left, whereas they are oriented vertical and horizontal on the right. Apparently, magneto-crystalline anisotropy

forces the antiferromagnetic axis $\vec{A}$ parallel or perpendicular to the crystallographic c-axis, explaining the vanishing contrast on the left ($\angle(\vec{A},\vec{E}) = \pm 45°$) and the strong contrast on the right ($\angle(\vec{A},\vec{E}) = 0°\, or\, 90°$). The antiferromagnetic configuration is displayed at the bottom of Fig. 2. From an analysis of not-spatially resolved spectroscopic data (not shown), we deduce, that $\vec{A}$ is inclined by 45° to the sample surface. Since in our experimental geometry $\vec{E}$ lies in the surface plane we cannot distinguish domains whose axis $\vec{A}$ is rotated by 180° about the surface normal. Thus we only observe two of the four antiferromagnetic domains that have to exist by symmetry.

Magnetic exchange coupling at the interface between an antiferromagnet and a ferromagnet is expected to cause corresponding domain configurations in both layers. We have investigated the domain structure in a Co wedge, grown on top of $LaFeO_3$ with a thickness ranging from 8 Å up to 25 Å, which was coated with 10 Å Pt to prevent oxidization. The probing depth of photoelectron emission microscopy using low-energy secondary electrons (20-50 Å) permits imaging of the $LaFeO_3$ and Co layers at the same time. The elemental specificity of x-ray absorption techniques furthermore allows distinguishing both layers, by acquiring images at the characteristic absorption resonances. In Fig. 3 the Co ferromagnetic and $LaFeO_3$ antiferromagnetic domain structure, acquired at exactly the same position, are shown together. The Co ferromagnetic configuration was imaged applying x-ray magnetic circular dichroism (XMCD) contrast, by dividing images acquired at the Co L_3 and at the Co L_2-edge using circularly polarized x-rays. The $LaFeO_3$ antiferromagnetic configuration was imaged using XMLD contrast, as explained above. The images show a clear correspondence of

the domain structures. On the left, two colors appear in the LaFeO$_3$ magnetic image representing the two AFM domains with orthogonal orientation of the antiferromagnetic axis that we are able to distinguish. Strong contrast arises between domains with the antiferromagnetic axis $\vec{A}$ parallel and perpendicular to the electric field vector $\vec{E}$, which is horizontal. Three colors in the Co XMCD image on the right correspond to four different directions of the magnetization vector $\vec{M}$. Using circularly polarized light, ferromagnetic domains with an opposite projection of $\vec{M}$ on the x-ray polarization $\vec{\sigma}$ can be distinguished. They appear bright in case of parallel orientation ($\vec{M}$ down) and dark in case of antiparallel orientation ($\vec{M}$ up). Domains with $\vec{M}$ pointing to the left and the right, orthogonal to the polarization $\vec{\sigma}$ appear in the same gray shade and are not differentiated in this image. These domains were resolved by a 90° rotation of the sample (not shown). Comparison of the in-plane projections of the AFM axis and the FM spin directions, illustrated above the images, reveals that the FM Co spins are always aligned parallel or antiparallel to the in-plane projection of the AFM axis. The correlation revealed by Fig. 3 is of magnetic rather than crystallographic origin since the Co layer is polycrystalline. The magnetic alignment of the Co domains, which exhibit an in-plane easy axis, must therefore be caused by a coupling to uncompensated spins at the LaFeO$_3$ surface with an in-plane component parallel to the in-plane projection of the AFM axis. Experiments to directly image this ferromagnetic component were unsuccessful on this system, probably because of their small concentration or magnitude.

In Fig. 4 the Co FM domain structure and the LaFeO$_3$ AFM domain structure are shown for different Co thickness. All images show magnetic domains of comparable size and the

described correspondence between the magnetic configuration of the FM and the AFM layer. As expected, the intensity originating from the buried $LaFeO_3$ layer decreases with Co thickness whereas the intensity from the Co layer increases. However, imaging through a 30 Å thick cap layer is still possible. The variation of the image contrast does not signify a modification of the magnetic moment with Co thickness. It is caused by the change of the peak-jump to background ratio of the Fe or Co resonances with Co layer thickness.

Investigations of the magnetization reversal process in the ferromagnetic layer have been carried out to quantify the coupling strength at the AFM – FM interface. A sequence of Co XMCD images was acquired after applying various magnetic fields, Fig. 5. The measurements were performed on a 25 Å Co / $LaFeO_3$(001) sample. The field was applied along the in-plane projection of the x-ray propagation (see Fig. 1) and microscopic XMCD images were acquired in zero-field, because of the deflection of electrons in a magnetic field. The images show that the magnetization reversal occurs by the switching of individual domains, whose magnetization direction and shape are defined by exchange coupling to the $LaFeO_3$ layer, and not by domain wall motion. The images also reveal a strong uniaxial anisotropy of the Co domains. Only Co domains that are coupled to $LaFeO_3$ domains with a projection of the AFM axis parallel to the field can be reversed (black to white) while orthogonal Co domains (gray) follow a hard axis loop and remain unchanged even after applying a field of more than 200 Oe. We furthermore observe a local unidirectional magnetic anisotropy of single Co domains, a local exchange bias. Local remanent hysteresis loops (Fig. 6), calculated from the field

dependent XMCD contrast in a sequence of images, show a repeatable loop shift of 30 Oe and more in single domains. This local bias is attributed to a surplus of uncompensated interface spins in the individual AFM domains which are frozen in after growth. Spatially averaged, the bias effects of individual domains cancel out, leading to the not shifted, averaged hysteresis loop, also shown in Fig. 6. The averaged loop exhibits only half of the XMCD brightness change because the orthogonal gray domains constitute half of the signal but do not switch. The lack of bias in the averaged loop is expected, because the studied sample was not set in a magnetic field. The setting procedure would shift the balance of the microscopically biased domains, resulting in a preferred macroscopic spin direction, i.e. macroscopic exchange bias.

Conclusion:

We have determined the magnetic structure of an antiferromagnet / ferromagnet bilayer, in particular of the system Co / $LaFeO_3$. The antiferromagnetic domain structure in a thin film sample has been resolved for the first time, using x-ray photo-electron emission microscopy. We have also investigated the magnetic interaction at the Co / $LaFeO_3$ interface. Magnetic exchange coupling across the interface causes a clear correspondence of the FM and the AFM domain structure in both layers. Investigation of the magnetization reversal process allowed quantifying the local bias field in single domains. We believe that x-ray absorption microscopy may hold the key to a definite understanding of the ferromagnet – antiferromagnet exchange bias phenomenon.

Acknowledgement:

Figures:

Fig. 1   Images acquired at 721.5 eV (A) and 723.2 eV (B) at the Fe L_2 edge using linearly polarized x-rays show the antiferromagnetic domain structure of $LaFeO_3$. The domain contrast at energy B is reversed to that at A. In the divided image A/B, referred to as the XLMD image, contrast of non-magnetic origin (topography, chemical composition) is surpressed. Local spectra measured within a dark and a bright domain show the origin of the image contrast: The branching ration between two multiplet peaks at the L_2-edge changes, because of the different angle between the x-ray polarization vector and the antiferromagnetic axis in each domain. The measurement geometry is also shown.

Fig. 2   The domain structure at the junction of a $LaFeO_3$ bi-crystal is shown. The crystal lattice is rotated by 45° at the boundary, indicated by black arrows, accompanied by a similar rotation of the antiferromagnetic axis. The photon polarization is horizontal. The relation between the magnetic configuration and the crystallographic structure is shown at the bottom.

Fig. 3   AFM domains in $LaFeO_3$ (left) and ferromagnetic domains in Co (right) were imaged exactly at the same position. Different colors signify a different direction of the magnetic vector, as indicated above the images.

Fig. 4   Thickness dependence of the FM (top) and the AFM (bottom) domain contrast in a $LaFeO_3$/Co bi-layer, coated with Pt.

Fig. 5 XMCD images of the FM domain structure. The images were acquired in remanence after applying magnetic fields in the sample plane.

Fig. 6 Remanent hysteresis loops calculated from the XMCD intensity in two selected domains, which have opposite bias. The average loop shows the XMCD intensity averaged over a multi-domain region.

References:

D. Alders, L. H. Tjeng, F. C. Voogt *et al.*, (1998). Phys. Rev. B **57**, 11623-11631.

S. Anders, H. A. Padmore, R. M. Duarte *et al.*, (1999). Rev. Sci. Instrum. **70**, 3973-3981.

A. E. Berkowitz & K. Takano, (1999). J. Magn. Magn. Mater. **200**, 552-570.

A. Fert, P. Grünberg, A. Barthelemy *et al.*, (1995). J. Magn. Magn. Mater. **140-144**, 1-8.

U. Gradmann, (1991). J. Magn. Magn. Mater. **100**, 481-496.

J. B. Kortright, D. D. Awschalom, J. Stöhr *et al.*, (1999). J. Magn. Magn. Mater. **207**, 7-44.

P. Kuiper, B. G. Searle, P. Rudolf *et al.*, (1993). Phys. Rev. Lett. **70**, 1549-1552.

J. P. Locquet, A. Catana, A. E. Machler *et al.*, (1994). Appl. Phys. Lett. **64**, 372-374.

J. P. Locquet, J. Perret, J. Fompeyrine *et al.*, (1998). Nature **394**, 453-456.

J. Nogues & I. K. Schuller, (1999). J. Magn. Magn. Mater. **192**, 203-232.

F. Nolting, A. Scholl, J. Stöhr *et al.*, (2000). Nature **405**, 767-769.

C. M. Schneider, P. Bressler, P. Schuster *et al.*, (1990). Phys. Rev. Lett. **64**, 1059-1062.

A. Scholl, J. Stöhr, J. Lüning *et al.*, (2000). Science **287**, 1014-1016.

J. Stöhr, (1999). J. Magn. Magn. Mater. **200**, 470-497.

J. Stöhr, A. Scholl, T. J. Regan *et al.*, (1999). Phys. Rev. Lett. **83**, 1862-1865.

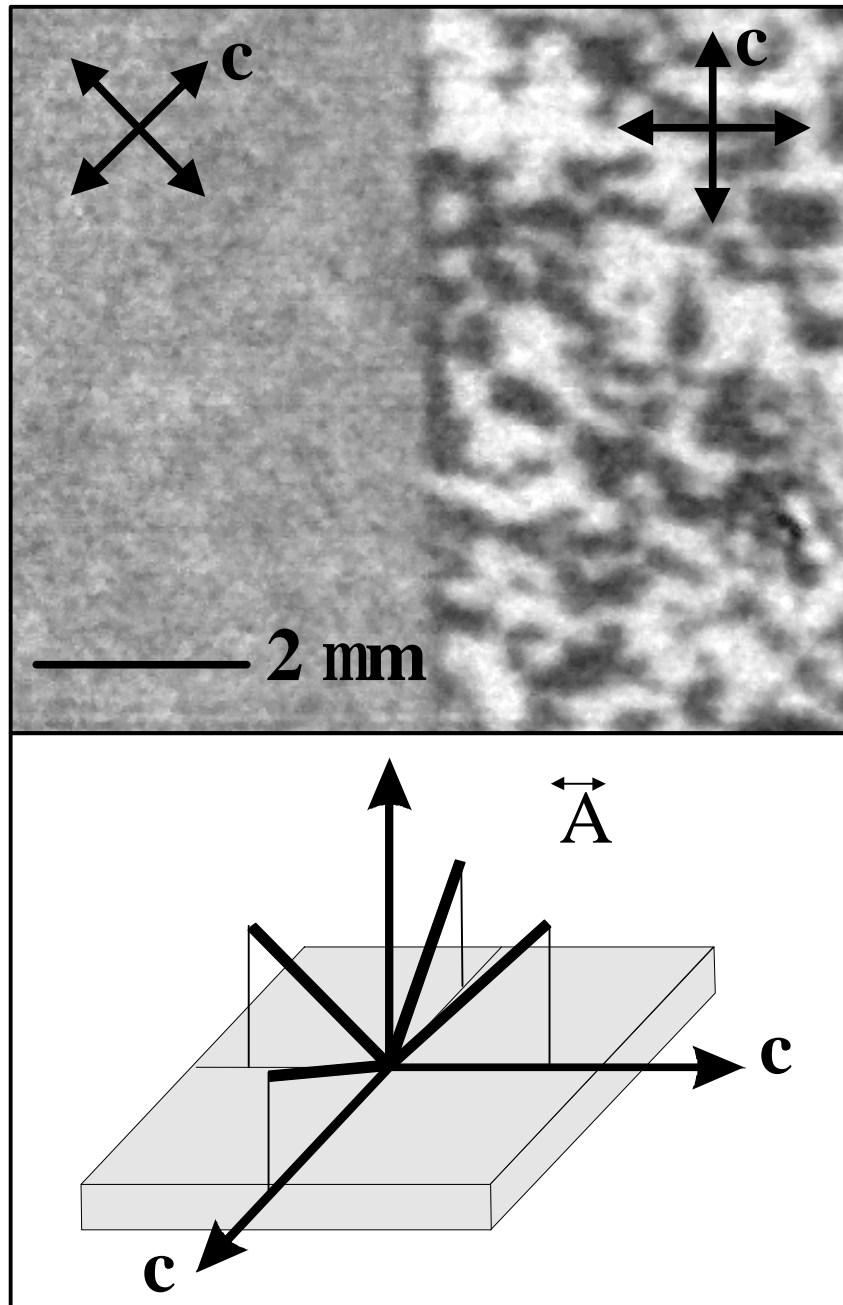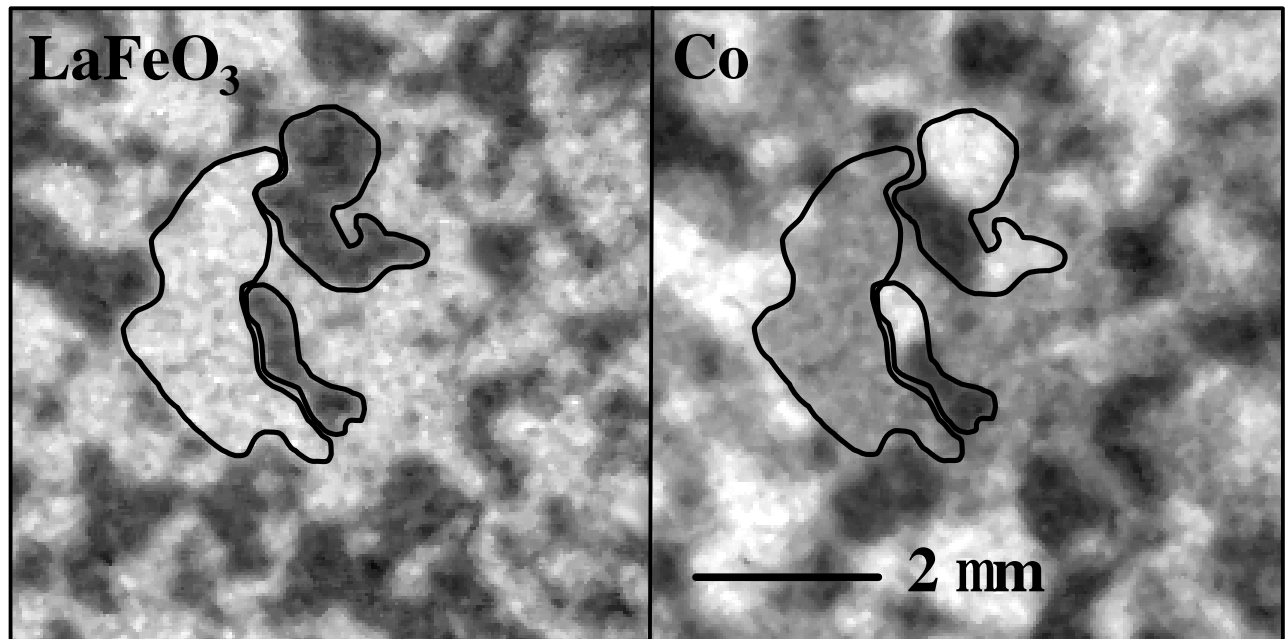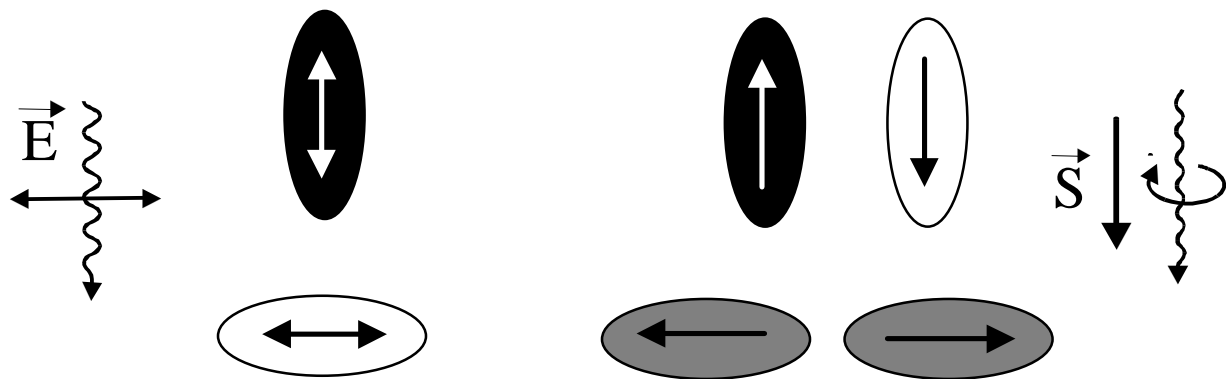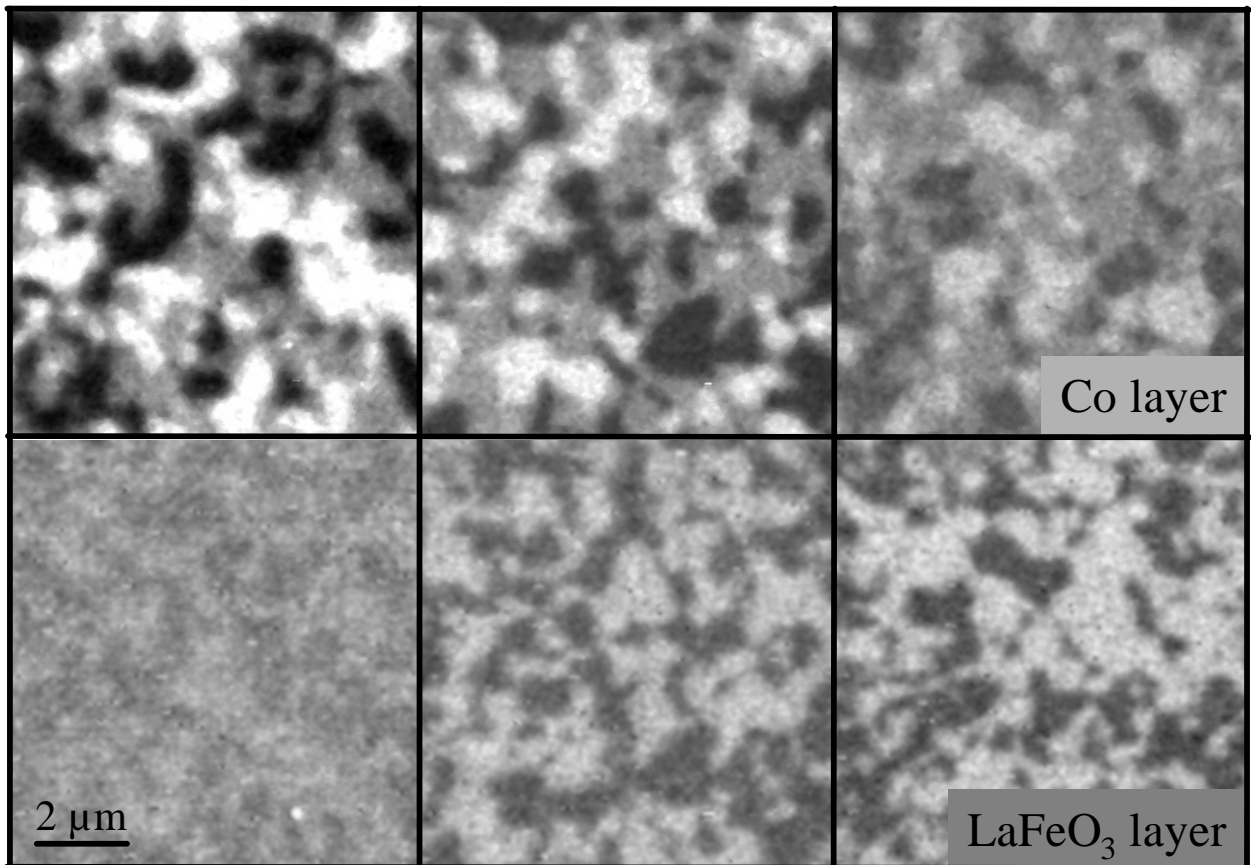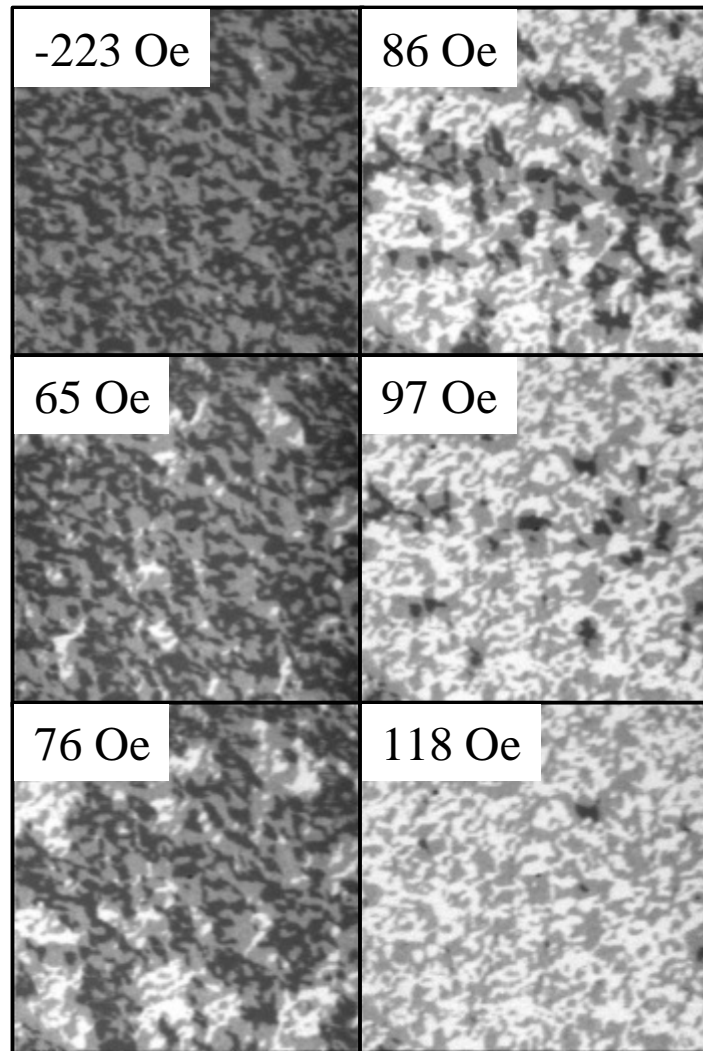A. Scholl
Fig. 1
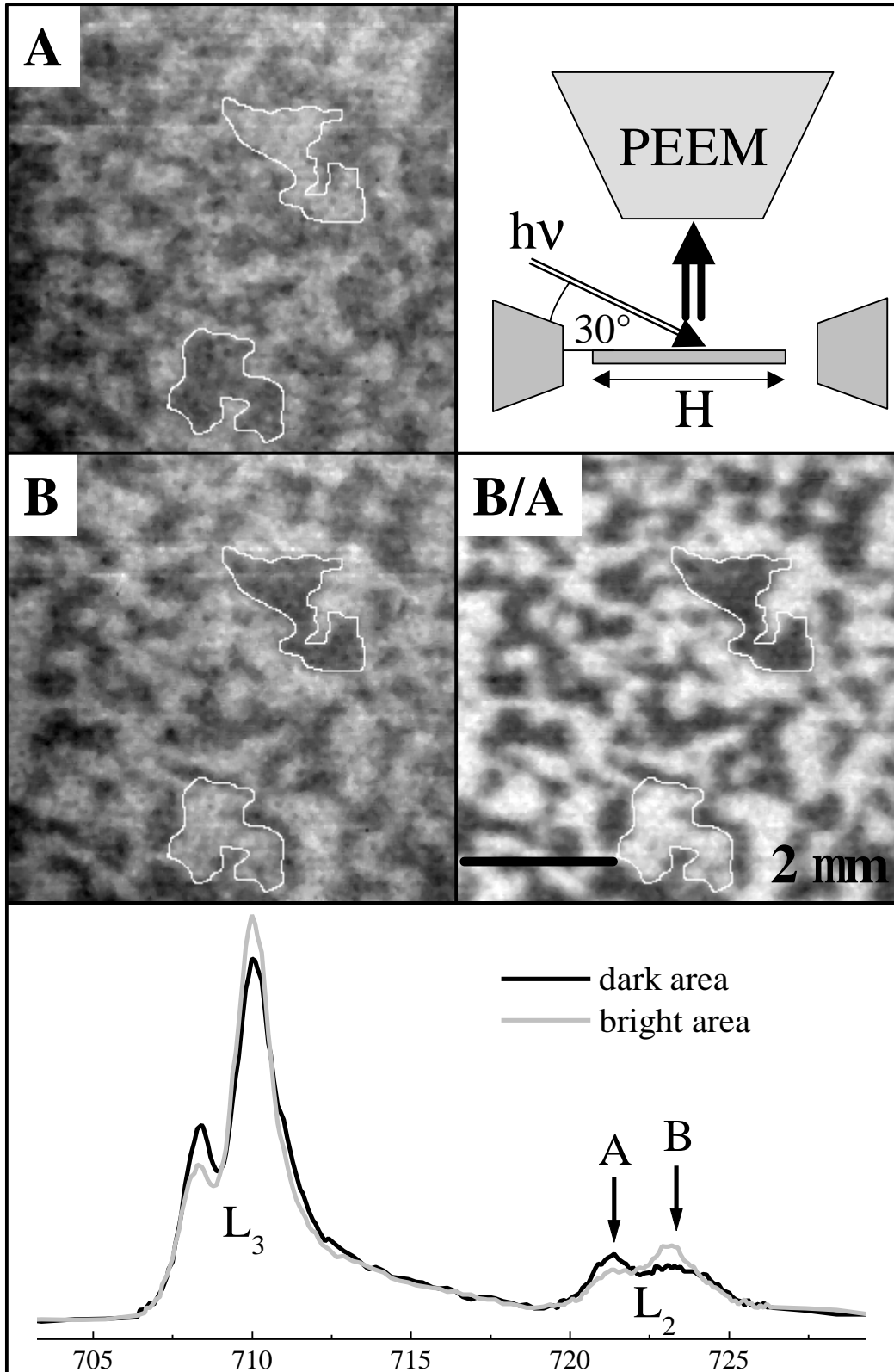
A. Scholl
Fig. 2

A. Scholl
Fig. 3

LaFeO₃

Co

2 mm

A. Scholl

Fig. 4

A. Scholl
Fig. 5

A. Scholl
Fig. 6